

Two-dimensional optical chimera states in an array of coupled waveguide resonators

M.G. Clerc,¹ S. Coulibaly,² M.A. Ferré,¹ and M. Tlidi³

¹*Departamento de Física and Millennium Institute for Research in Optics, Facultad de Ciencias Físicas y Matemáticas, Universidad de Chile, Casilla 487-3, Santiago, Chile*

²*Université de Lille, CNRS, UMR 8523-PhLAM-Physique des Lasers Atomes et Molécules, F-59000 Lille, France*

³*Faculté des Sciences, Université Libre de Bruxelles (U.L.B), CP 231, Campus Plaine, B-1050 Bruxelles, Belgium*

(Dated: 24 December 2019)

Two-dimensional arrays of coupled waveguides or coupled microcavities allow to confine and manipulate light. Based on a paradigmatic envelope equation, we show that these devices, subject to a coherent optical injection, support coexistence between a coherent and incoherent emission. In this regime, we show that two-dimensional chimera state can be generated. Depending on initial conditions, the system exhibits a family of two-dimensional chimera states and interaction between them. We characterize these two-dimensional structures by computing their Lyapunov spectrum, and Yorke-Kaplan dimension. Finally, we show that two-dimensional chimera states are of spatiotemporal chaotic nature.

One-dimensional nonlinear coupled microcavities exhibit a rich spatiotemporal dynamics. In particular, these coupled microcavities have fully synchronized or incoherent light emission of a spatiotemporal chaotic nature. Also, depending on the initial conditions, these devices show coexistence between desynchronized and synchronized domains, often called *optical chimera states*. In this contribution, we show evidence of optical chimeras in a two-dimensional array of coupled waveguide resonators. Due to the additional degrees of freedom, the smaller localized solutions exhibit a chaotic spatiotemporal evolution—which is not the case of the one-dimensional counterpart. Lyapunov spectrum and Yorke-Kaplan dimensions are calculated to characterize these intriguing localized states.

*chimera states*¹³. Initially, this phenomenon was reported in the context of nonlocally coupled phase oscillators^{13,14}, and extended later on to locally coupling oscillators^{15,16}. In optical systems, experimental observations of chimera states have been reported using an optoelectronic delayed feedback setup¹⁷, laser diodes coupled to a nonlinear saturable absorber¹⁸, and laser diodes subjected to a coherent polarization¹⁹. Recently, one-dimensional optical chimera states have been predicted in an array of coupled Kerr resonators²⁰. However, to the best of our knowledge chimera states in two spatial dimensions have received limited attention²¹.

This paper aims to investigate the formation of two-dimensional optical chimera states in an array of coupled waveguide resonators. This phenomenon occurs in a regime where a coupled waveguide resonators exhibit a coexistence between a coherent and incoherent emission. These discrete structures consist of a localized complex domain embedded in a stable homogenous background. To account for 2D optical chimera states, we use a discrete version of the two-dimensional Lugiato-Lefever equation²². Based on this model, we show that, depending on the initial condition; this system can support a family of two-dimensional optical chimera states. Lyapunov exponents and Yorke-Kaplan dimension allow characterizing these structures. Chimera states correspond to localized spatiotemporal chaos. In the Lugiato-Lefever equation, the optical chimera states are excluded. Indeed, this dynamical behavior is a peculiarity of discrete systems.

I. INTRODUCTION

A two-dimensional array of coupled waveguides or coupled microcavities consists of nonlinear discrete structures¹. This configuration appears not only in photonics but also in a large variety of systems such as biological systems², condensed matter physics³, and Bose-Einstein condensates⁴. Nonequilibrium discrete systems are drawing considerable attention both from fundamental as well as applied points of view. In particular, spatial localization of light in discrete photonic lattices has been reported⁵⁻⁷, including complex confinement of light such as random-phase solitons^{8,9}. In free propagation, the spatial confinement is attributed to the balance between the discrete diffraction and the nonlinearity. However, when dealing with coupled microresonators, the dissipation of energy due to mirrors should be compensated by optical injection. This second balance renders discrete dissipative solitons more robust¹⁰⁻¹².

Generally speaking, when a system exhibits a simultaneous coexistence between coherence and incoherence behavior in coupled oscillators, the resulting phenomenon is called

II. ARRAY OF DRIVEN COUPLED WAVEGUIDE RESONATORS: 2D DISCRETE LUGIATO-LEFEVER MODEL

Let us consider a two-dimensional square array of coupled waveguide resonators subject to a coherent monochromatic beam. Figure 1 shows a schematic representation of the driven square lattice. Each resonator is composed of a waveguide filled by a Kerr media, with dielectric mirrors at

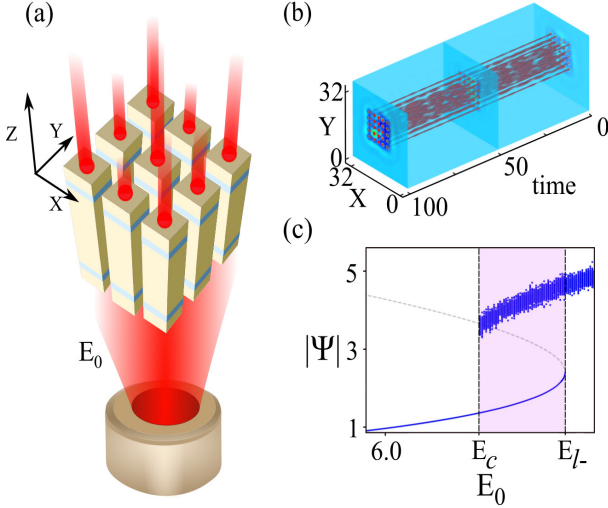


FIG. 1. Optical chimera states in a two-dimensional array of coupled microresonator. Parameters are $E_0 = 4.22$, $\Delta = -0.506$, and $\kappa = 1.876$. (a) Schematic representation of a two-dimensional array of coupled-waveguide resonators driven by an external field of intensity E_0 . (b) Spatiotemporal evolution of the maximum isosurface amplitude of each interacting cavity. (c) Bifurcation diagram of model Eq. (1). The total intracavity amplitude $|\Psi|$ as function of the pump amplitude E_0 . The solid and dashed lines describe the total intracavity intensity of homogeneous steady states. The blue cloud of points shows the extreme values of the total intracavity intensity of the spatiotemporal chaotic state. The colored region accounts for the coexistence range ($E_c = 6.68 < E < E_{l-} = 7.29$). 2D optical chimera states are observed inside this interval.

the end-faces. Indeed, this system corresponds to a lattice of waveguide microcavities. This device can be described by the discrete Lugiato-Lefever model^{11,12}. Note that this prototype model of driven coupled oscillators has been more studied in the one-dimensional configuration. Assuming that the coupling between waveguide-resonators is small in comparison with the cavity size, the intracavity field satisfies

$$\partial_T \Psi_{n,m} = E_0 - (1 + i\Delta)\Psi_{n,m} - i|\Psi_{n,m}|^2\Psi_{n,m} - i\kappa(\Psi_{n+1,m} + \Psi_{n-1,m} + \Psi_{n,m+1} + \Psi_{n,m-1}), \quad (1)$$

where $\Psi_{n,m}(T)$ is a slowly varying envelope of the electric field circulating in (n,m) -coupled resonators. Indices n (x -axis) and m (y -axis) denote the transverse coordinates of the cavities. The detuning parameter $\Delta \equiv \omega - \omega_0$ is proportional to the difference between the resonance frequency ω_0 of the cavity and the driving field frequency ω . κ characterizes the coupling strength between the cavities. The time $t = T\tau_{ph}$ is measured in the photon lifetime unit τ_{ph} . The driving field intensity is denoted by E_0 . The continuous counterpart of model Eq. (1) was used to describe Kerr optical frequency combs (see the special issue²³ and references therein).

In the continuous limit, for $\Delta > \sqrt{3}$ ($\Delta < \sqrt{3}$), the transmitted intensity as a function of the input intensity E_0^2 is bistable (monostable). The homogeneous steady state undergoes a modulational instability at $E_0^2 = E_{0c}^2 \equiv 1 + (1 - \Delta)^2$ and $|\Psi_c|^2 = 1$. At this bifurcation point, the critical wave-

length is $\Lambda_c^2 = [2\pi|\kappa|/(2 - \Delta)]^{1/2}$. It has been shown that, for large injected intensity, the system exhibits a spatiotemporal chaos²⁴. These dynamic behaviors are persistent when one considers the respective discrete system²⁰. In this type of systems, the discreteness (Peierls-Nabarro potential) allows the confinement of light. Hence, the prerequisite condition for the formation of two-dimensional chimera states is the coexistence of a coherent (homogeneous state) and an incoherent state (spatiotemporal chaos) in a discrete system. Figure 1b displays a typical 2D chimera state in the bistability region, $E_c < E_0 < E_{l-}$. Chimera states are classified by the notation $n \times m$, which depicts the number of cavities that shows the maximum amplitude. Numerical simulations are conducted using a finite difference code with a 4th-order Runge-Kutta scheme and Neumann boundary conditions. Contrary to the continuous limit, the 2D chimera states neither grow in spite of available free space in the transverse plane nor shrink in spite of weak coupling between resonators. Figure 1c shows the bifurcation diagram of model Eq. (1). We plot the maximum values of the normalized total intracavity amplitude $|\Psi|$ as a function the injected field amplitude E_0 . The normalized total amplitude of the intracavity field is defined as, $|\Psi(t)| = \sqrt{\sum_{i,j=1}^N |\Psi_{i,j}(t)|^2}/N^2$ with N^2 is the total number of coupled cavities in the lattice.

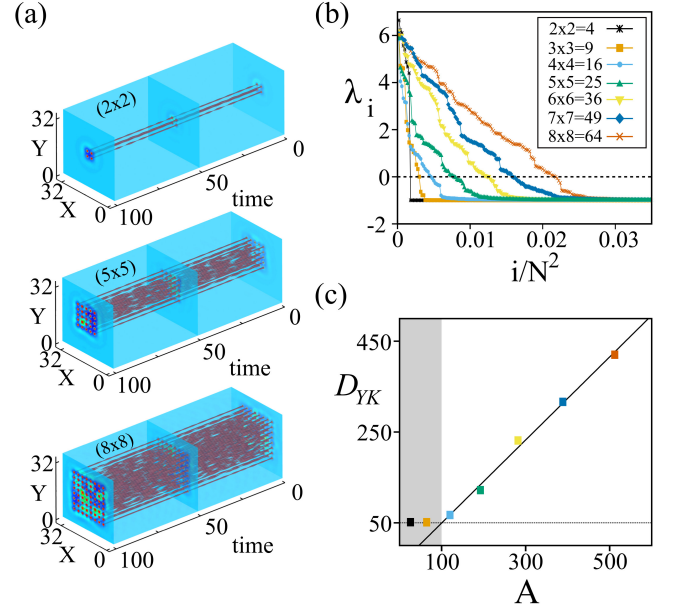


FIG. 2. Family of two-dimensional optical chimera states of model Eq. (1) with the same parameters as (a) Spatiotemporal diagrams of 2×2 , 5×5 , and 8×8 optical chimera states. The product $n \times m$ accounts for the number of cavities that shows the maximum amplitude. (b) Lyapunov spectra of different 2D optical chimera states obtained from Eq. (1). $\{\lambda_i\}$ denotes the i -Lyapunov exponent, $i = \{1, \dots, N\}$, and N accounts for the total number of cavities. Each curve corresponds to the Lyapunov spectrum of the respective $n \times m$ chimera states. (c) Yorke-Kaplan dimension of the spatiotemporal chaotic solution as function of A parameter. This parameter accounts for the average number of microcavities in the incoherence domain.

For small E_0 , only a homogeneous steady state exists as a stable solution. In this case, all cavities have the same intracavity field amplitude. Increasing the input parameter up to $E_0 \geq E_{l-}$, the homogeneous steady state suffers a saddle-node instability. The system develops the emergence of spatiotemporal chaos²⁴. Further increasing E_0 , the complex dynamics keeps up. When decreasing E_0 , the spatiotemporal complex dynamics perseveres until E_0 reaches E_c (see Fig. 1c). For $E_0 < E_c$, the homogeneous steady state is the only extended stationary equilibrium. Indeed, the system presents a subcritical bifurcation at $E_0 = E_c$. The coexistence is prerequisite for the formation scenario of chimera states we have previously proposed in 1D¹⁵.

The first finding is that the family of chimera states generated in the transverse section of the intracavity field is much more diverse than one-dimensional case, thanks to the large variety of 2D geometrical plots. However, for the sake of simplicity, we limit our analysis to chimera states with incoherent domains forming a square as depicted in Figure 2a. These chimera states are characterized by spatial confinement of large temporal fluctuations (see video in supplement).

III. CHARACTERIZATION OF 2D OPTICAL CHIMERA STATES

In dynamical systems theory, Lyapunov exponents constitute the most adequate tool to characterize the nature of complex spatiotemporal dynamics described above. These exponents provide information about sensitivity to the initial conditions, fluctuations, and complexity of solutions²⁵. Low dimensional and spatiotemporal chaos are characterized by positive Lyapunov exponents. These exponents can be computed from the method proposed by Skokos²⁶. The set of Lyapunov exponents constitutes the Lyapunov spectrum $\{\lambda_i\}$ with $i = \{1, 2, \dots, N^2\}$, $\lambda_i \leq \lambda_j$, and $i \leq j$. Low-dimensional chaos possesses a discrete Lyapunov spectrum, while spatiotemporal chaos has a continuous one. Figure 2b shows Lyapunov spectra of different optical chimera states. From this plots, we see that positive Lyapunov exponents increase with the size of chimera states. Hence, the complexity of these localized solutions increase with chimera states size.

In addition, from Lyapunov spectrum we can compute the Yorke-Kaplan dimension defined by $D_{YK} = p + \sum_{i=1}^p \lambda_i / |\lambda_{p+1}|$, where p is the largest integer for which $\lambda_1 + \dots + \lambda_p > 0$. Figure 2c shows the Yorke-Kaplan dimension of different chimera solutions. From small values of A , the Yorke-Kaplan dimension remains constant, where A denotes the average number of microcavities in the incoherence domains. As A is increased the Yorke-Kaplan dimension grows. This feature is the manifestation of extensive property of this dynamical dimension²⁵, indicating that 2D optical chimera states belong to the class of spatiotemporal chaos.

Fourier analysis is used to further characterize the underlying dynamics of chimera states. To perform this analysis, we have the spectral density of the signal recorded at the location of one of the largest local maxima in the incoherent domain. Figure 4 shows the resulting power spectrum for

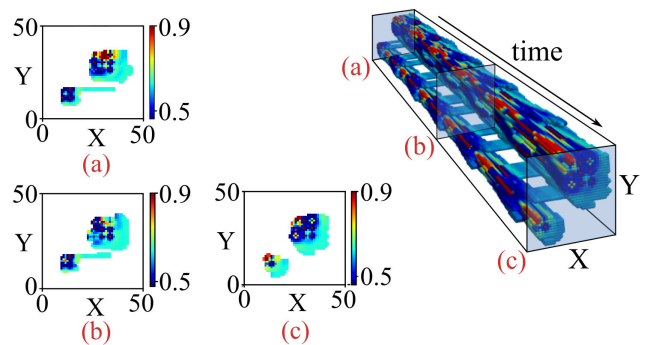


FIG. 3. 2D chimera states exist together. Spatiotemporal diagram of 2D chimera states in an array of coupled waveguide-resonator cavities. The color bar stands for the intracavity intensity field. Insets (a), (b), and (c) account for the cross section at different time.

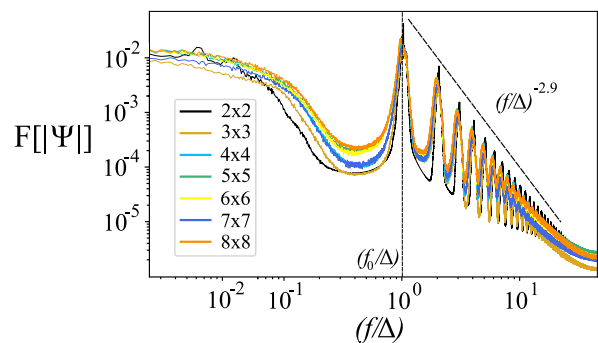


FIG. 4. Power spectrum $F[|\Psi|]$ of a single waveguide-resonator cavity as function of the frequency f and the detuning parameter Δ . At high frequencies, the power spectrum shows a power law $f^{-2.9}$ which is a signature of turbulence-like dynamics.

different chimera states. The shape of the power spectrum is not affected by the size of the incoherence domain. The power spectrum has a dominant peak at the value of the detuning parameter. For high frequencies, the power spectrum presents a power f^n where $n = -2.932$, which is a signature of turbulence-like behavior²⁷.

Finally, numerical simulations of model Eq. (1) shows evidence of the coexistence between dissimilar chimera states simultaneously in different spatial locations in the transverse plane. An example of such a behavior is shown in Fig. 3, where 2×2 and 3×3 optical chimera states exist together. Insets account for the cross section at different times. The 2D spatiotemporal diagram suggest that the chimera states interact weakly.

IV. CONCLUSION

We have shown evidence of two-dimensional optical chimera states in a driven array of locally-coupled passive Kerr optical resonators. Adequate initial conditions have been used to generate a family of these solutions. The main characteristic of these solutions is spatial confinement of light in

the transverse plane involving complex multi-peaks dynamics. Besides, we have shown that these solutions can coexist together. The 2D chimera states are inherent to the discrete nature of the system. Indeed, in the continuous limit, these states are unstable. We have characterized these solutions by computing Lyapunov spectra, York-Kaplan dimensions, and power spectrum. We have showed that the 2D optical chimera states belong to the class of spatiotemporal chaos and turbulence like behaviors. The prerequisite condition for their formation requires a bistable behavior between homogeneous background and spatiotemporal chaos. This condition is rather general, and therefore, this prediction is important for the identification and understanding of the various complex spatiotemporal behaviors observed in practical systems.

SUPPLEMENTARY MATERIAL

See supplement for supporting contents

ACKNOWLEDGMENTS

M.G.C. and M.A.F. acknowledge the financial support of Millennium Institute for Research in Opticsan Fondecyt 1180903. M.T. is a Research Director of the Fonds National de la Recherche Scientifique (Belgium).

¹D. N. Christodoulides and R. I. Joseph, *Opt. Lett.* **13**, 794 (1988).

²A. S. Davydov and N. I. Kislukha, *Phys. Status Solidi B* **59** 465-470 (1973).

³W. P. Su, J. R. Schieffer and A. J. Heeger, *Phys. Rev. Lett.* **42**,1968-1971 (1979).

⁴A. Trombettoni and A. Smerzi, *Phys. Rev. Lett.* **84**, 5435-5438 (2001).

⁵D. N. Christodoulides, F. Lederer, and Y. Silberberg, *Nature* **424**, 817 (2003); R. Morandotti, U. Peschel, J. S. Aitchison, H. S. Eisenberg, and Y. Silberberg, *Phys. Rev. Lett.* **81** 3383

⁶Fleischer, J. W., Segev, M., Efremidis, N. K., and Christodoulides, D. N. (2003). *Nature*, 422(6928), 147.; N. K. Efremidis, S. Sears, D. N. Christodoulides, J. W. Fleischer, and M. Segev, *Phys. Rev. E* **66**

046602 (2002); D. Neshev, E. Ostrovskaya, Y. Kivshar, and W. Krolikowski, *Opt. Lett.* **28**, 710 (2003)

⁷A. Fratalocchi, G. Assanto, K. A. Brzdakiewicz, and M. A. Karpierz, *Opt. Lett.* **29**,1530 (2004); Y. V. Kartashov, V. A. Vysloukh, *Opt. Lett.* **30**, 637 (2005); H. Martin, E. D. Eugenieva, Z. Chen, and D. N. Christodoulides, *Phys. Rev. Lett.* **92** 123902 (2004); B. A. Malomed and P. G. Kevrekidis, *Phys. Rev. E* **64**, 026601 (2001)

⁸O. Cohen, G. Bartal, H. Buljan, T. Carmon, J. W. Fleischer, M. Segev, and D. N. Christodoulides, *Nature* **433**, 500 (2005)

⁹H. Buljan, O. Cohen, J. W. Fleischer, T. Schwartz, M. Segev, Z. H. Muslimani, N. K. Efremidis, and D. N. Christodoulides, *Phys. Rev. Lett.*, **92**, 223901 (2004).

¹⁰U. Peschel, O. Egorov, Lederer, *Opt. Lett.* **29** 1909 (2004).

¹¹O. Egorov, U. Peschel, and F. Lederer, *Phys. Rev. E* **71**, 056612 (2005).

¹²O. A. Egorov and F. Lederer, *Opt. Lett.* **38**, 1010 (2013).

¹³D. M. Abrams and S. H. Strogatz, *Phys. Rev. Lett.* **93**, 174102 (2004).

¹⁴Y. Kuramoto and D. Battogtokh, *Nonlinear Phenom. Complex Syst.* **5**, 380 (2002)

¹⁵M. G. Clerc, S. Coulibaly, M. Ferré, M. A. García-Núñez, and R. G. Rojas, *Phys. Rev. E* **93**, 052204 (2016).

¹⁶M.G. Clerc, S. Coulibaly, M.A. Ferré, and R.G. Rojas, *Chaos*, **28**, 083126 (2018).

¹⁷L. Larger, B. Penkovsky, and Y. Maistrenko, *Nat. Comm.* **6**, 7752 (2015).

¹⁸E. A. Viktorov, T. Habruseva, S. P. Hegarty, G. Huyet, and B. Kelleher, *Phys. Rev. Lett.* **112**, 224101 (2014).

¹⁹C.-H. Uy, L. Weicker, D. Rontani, and M. Sciamanna, *APL Photon.* **4**, 056104 (2019).

²⁰M. G. Clerc, M. A. Ferré, S. Coulibaly, R. G. Rojas, and M. Tlidi, *Opt. Lett.* **42**, 2906 (2017).

²¹K. M. Aghdami, M., Golshani, and R. Kheradmand, *IEEE Photonics journal*, **4**, 1147 (2012).

²²L. A. Lugiato and R. Lefever, *Phys. Rev. Lett.* **58**,2209 (1987).

²³Y.K. Chembo, D. Gomila, M. Tlidi, and C.R. Menyuk, *Eur. Phys. J. D* **71**, 299 (2017).

²⁴Z. Liu, M. Ouali, S. Coulibaly, M.G. Clerc, M. Taki, and M. Tlidi, *Opt. Lett.*, **42**, 1063 (2017).

²⁵A. Pikovsky and A. Politi, *Lyapunov Exponents: A Tool to Explore Complex Dynamics* (Cambridge University, 2016).

²⁶C. H. Skokos, "The Lyapunov characteristic exponents and their computation", in *Dynamics of Small Solar System Bodies and Exoplanets* (Springer, 2010), pp. 63–135.

²⁷U. Frisch, and A. N. Kolmogorov, *Turbulence: the legacy of AN Kolmogorov* (Cambridge university press, 1995).